

THE HALO AND MAGNETIC FIELD OF THE COMA CLUSTER OF GALAXIES

K.-T. KIM AND P. P. KRONBERG

Department of Astronomy, University of Toronto

AND

P. E. DEWDNEY AND T. L. LANDECKER

Dominion Radio Astrophysical Observatory, National Research Council of Canada

Received 1988 December 22; accepted 1989 November 27

ABSTRACT

New observations of the radio emission from the Coma Cluster of galaxies have revealed the most detailed image of an intergalactic halo yet seen in a cluster of galaxies. The centroid of the halo emission is significantly displaced from that of the X-ray emission. The Faraday rotation of polarized emission from background radio sources has been measured. There is a significant contribution to the rotation measure (RM) of sources seen through the cluster. The excess RM, when combined with the X-ray data, has allowed us to make the first direct measurement of the magnetic field strength in the Coma Cluster. This measurement, about $2 \mu\text{G}$, provides an independent check of the widely used assumption of equipartition between the energy in relativistic particles and that in the magnetic field. Our observations also allow an estimate of the degree of tangling of the cluster magnetic field. The magnetic field reversals seem to occur on a scale size of 13–40 kpc. The extent of the halo emission and the degree of field tangling indicate that the radio halo source must be sustained by particle reacceleration in the intracluster medium.

Subject headings: galaxies: clustering — galaxies: intergalactic medium — galaxies: X-rays — magnetic fields — polarization — radio sources: galaxies

I. INTRODUCTION

The detailed morphology and physical parameters of the diffuse hot gas in galaxy clusters have been difficult to define because of the technical difficulties in detecting and imaging its very faint radiation. The relativistic and thermal components of intracluster gas contain important information about the effect of the intracluster medium (ICM) on the evolution both of the clusters and of their member galaxies. We would also like to understand how the relativistic gas component of intracluster gas is produced—clues to this puzzle lie in details of the radio and X-ray spectra and in the radio polarization. In the current paradigm, the X-ray emission from clusters is thermal in origin. Our purpose is to study the origin of the diffuse, nonthermal emission from clusters, detectable at radio wavelengths but not associated with individual galaxies. We use the term “halo” to denote such emission.

The existence of diffuse intracluster gas has been demonstrated from both radio and X-ray data for a number of the nearest rich clusters of galaxies (Willson 1970; Hanisch 1980). Of these, only a few Abell clusters have halo-type radio sources: Examples are the Coma Cluster, the Perseus Cluster (A426), which contains a halo of about $12'$ in diameter centered on 3C 84 (=NGC 1275) (Gisler and Miley 1979), A2255 (Harris, Kapahi, and Ekers 1980), A2256 (Bridle *et al.* 1979), A2319 (Harris and Miley 1978), and an irregular cluster A1367 (Gavazzi and Trinchieri 1983). Although these clusters contain an X-ray emitting ICM, their radio halos are patchy. Our analysis will suggest that this reflects their “localized” intracluster magnetic field.

The proximity of the Coma Cluster makes it a good “laboratory” for studying the physical conditions in intracluster gas in detail; the $1'$ angular resolution of our observations corresponds to 40 kpc for a Hubble constant of $50 \text{ km s}^{-1} \text{ Mpc}^{-1}$. However, even for the Coma Cluster, the properties of

its halo are known in less than adequate detail. This is partly because most radio telescopes tuned to relatively low radio frequencies (at which the radio halo is most prominent) have inadequate resolution or poorly known beam characteristics, or they are insensitive to the very large scale radio emission.

To overcome these limitations, we have used combined-array techniques which, although not new in themselves, are new to this class of problem. Specifically, we report the results of three observations of the Coma Cluster using the NRAO Very Large Array¹ (VLA) and the wide-field Synthesis Telescope at the Dominion Radio Astrophysical Observatory (DRAO).² The first observation (*a*) was to make wide-field, full-aperture synthesis maps of the Coma Cluster at 408 MHz with the DRAO Telescope, to which we added short baseline information taken by Haslam *et al.* (1982) with the 100 m Effelsberg antenna. (*b*) We also used the DRAO Telescope to conduct similar synthesis observations at 1420 MHz. To improve both the resolution and sensitivity of these observations, we used the NRAO VLA to make a deep map of Coma C at 1380 and 1630 MHz. The 1420 MHz DRAO data (which benefit from the wide angular field of the 9 m antennas) were then merged with the 1380 MHz VLA data (made with 25 m antennas) to combine the DRAO's sensitivity to the large-scale structure of the intracluster emission with the VLA's greater sensitivity at higher resolution.

The third phase of our project was (*c*) a successful detection of Faraday rotation in the Coma Cluster itself. The VLA was used to map 17 radio sources both toward and away from the Coma Cluster, in all Stokes parameters at four frequencies,

¹ The National Radio Astronomy Observatory is operated by Associated Universities, Inc., under contract with the National Science Foundation.

² The DRAO synthesis telescope is operated as a national facility by the National Research Council of Canada.

1465, 1665, 4835, and 4885 MHz. The results produced Faraday rotation measures (RMs) of 17 sources. By combining these data with those from the *Einstein* X-ray map of the Coma Cluster (Abramopoulos and Ku 1983), we obtain what is probably the most direct estimate of an intracluster magnetic field strength. (d) The fourth phase was a VLA search for polarized emission from the radio halo. This resulted in an upper limit that provides further information on the structure of the intracluster magnetic field.

We describe these results, discuss their implications, and show how they improve our knowledge of the physical processes at work in the gaseous component of clusters of galaxies.

II. RADIO OBSERVATIONS OF THE COMA CLUSTER OF GALAXIES

a) Radio Emission at 408 MHz

The Synthesis Telescope at DRAO (Roger *et al.* 1973; Veidt *et al.* 1985) can map structure at 408 MHz over the range of sizes from $3'.5$ to $3''$. Emission from larger structures is attenuated because the shortest baseline is 13 m. The missing information can be derived from single-antenna observations, and the data of Haslam *et al.* (1982) were used for this purpose. The resulting map is shown in Figure 1.

b) Radio Emission at 1.4 GHz

The 1420 MHz DRAO Synthesis Telescope map was produced by a similar technique, although in this case no single-antenna data were added. The resulting map is similar to that of Hanisch (1980), using the Arecibo radio telescope at 1420 MHz, and that of Schlickeiser, Sievers, and Thiemann (1987), using the 100 m Effelsberg telescope at 2700 MHz. This shows that, even without the addition of lower spatial frequency components, the DRAO telescope is capable of detecting the Coma halo.

To improve both the resolution and sensitivity of our 1420 MHz DRAO map, we made a deep map of Coma C at 1380

and 1630 MHz using the VLA. The experiment consisted of 9.5 hr of observing time on the Coma Cluster at each frequency, in addition to calibration time. The latter included 21 separate observations of the polarization calibrator, 3C 286, for which both the degree and direction of polarization are well known. The small angular separation of 3C 286 and the Coma Cluster allows us to remove ionospheric Faraday rotation accurately.

After careful data editing and image processing, we were able to generate a 1380 MHz map of the Coma Cluster with a dynamic range of 3000:1. This is close to the maximum possible, in which we have reduced all residual spurious features to a level of $30 \mu\text{Jy beam}^{-1}$, close to the thermal noise level. A similar image was made at 1630 MHz, but we did not achieve quite as good a dynamic range as at 1380 MHz.

Although the VLA observations combine high angular resolution, sensitivity, and precision, the sensitivity at spacings less than 25 m, the diameter of the VLA antennas, is reduced. The shortest interferometer spacings of the 9 m DRAO antennae generate the information on the broadest component of the Coma halo.

The final stage of mapmaking was to combine the data sets from the VLA (at 1380 MHz) and from the DRAO Synthesis Telescope (at 1420 MHz) in the Fourier transform plane. The resulting map was deconvolved using the CLEAN procedure. This map (Fig. 2) reveals both the small- and large-scale features of the Coma halo—the latter not being visible on the map made with the VLA alone. The size of the halo, as fitted with a two-dimensional elliptical Gaussian, is $18'.7 \times 13'.7$ with the major axis oriented at a position angle of 85° .

Our estimates for the total flux density and overall spectral index of the halo are based on the present data as well as flux densities taken from the literature. Flux densities of the halo measured at various wavelengths are summarized in Figure 3.

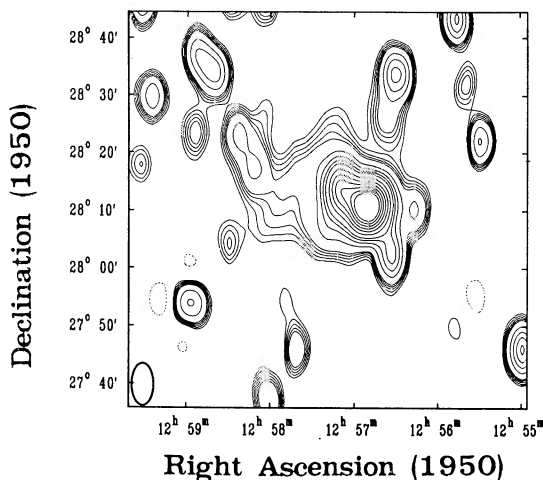


FIG. 1.—Full synthesis radio map of the Coma C region at 408 MHz, made with the DRAO telescope, after adding data from the Effelsberg 100 m telescope. The synthesised beam size (shown in the lower left corner) is 7.45×3.45 and the sensitivity is 8 mJy beam^{-1} . The central elongated peak is due to 5C 4.81 and 5C 4.85, and the extended emission which surrounds these is clearly seen. The overall shape of the radio halo at 408 MHz is primarily elongated west-east. The contour levels are at $-30, 40, 50, 60, \dots, 100, 200, \dots, 900 \text{ mJy beam}^{-1}$.

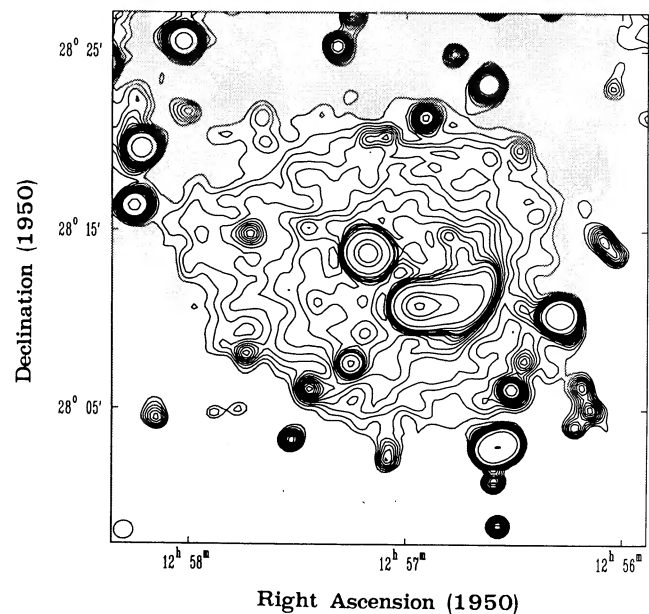


FIG. 2.—The contour map of the radio halo in the Coma Cluster of galaxies observed at 1.4 GHz. The radio halo is elongated E-W. The FWHM size of the radio halo is measured with a two-dimensional elliptical Gaussian fitting algorithm to give $18'.7 \times 13'.7$ elongated at $85^\circ.2$. Contours are shown at $-0.6, 1.2, 1.4, 1.6, \dots, 3.4, 4, 5, 10, 50, 100, 200 \text{ mJy beam}^{-1}$. The restoring beam is $71'' \times 60''$ elongated at $-85^\circ.5$.

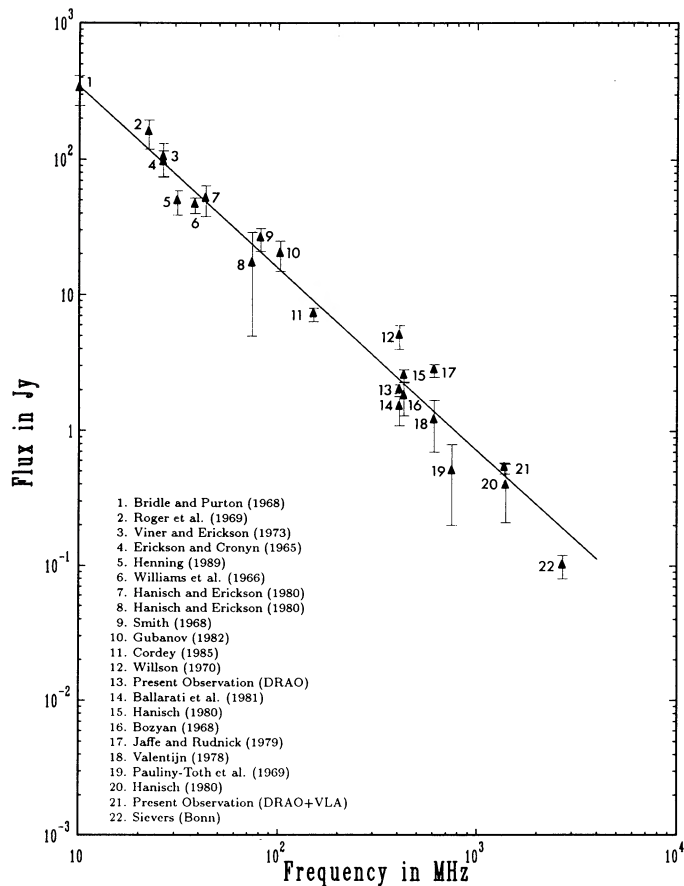


FIG. 3.—The best fit of the spectral index of the Coma radio halo is shown

They are 0.72 ± 0.13 Jy at 1 GHz and $\alpha = 1.34 \pm 0.06$ ($S \propto \nu^{-\alpha}$) for 10 MHz to 1400 MHz. There is no strong evidence for curvature on the spectrum. Recently, however, Schlickeiser, Sievers, and Thiemann (1987) have claimed that the total radio halo spectrum is steeper at frequencies above about 1400 MHz.

Note that the halo brightness distribution, after removal of small-diameter sources, is regular enough to be fitted meaningfully with an elliptical Gaussian. The brightness distribution at lower frequencies also shows a similar morphology. 5C 4.81 was removed from the halo (at 1' resolution) by approximating it as a Gaussian, and 5C 4.85 was removed by "blanking" it to the level of the diffuse emission around its boundary. We estimate the uncertainty in these removals to be less than 5% of the total halo flux density.

Since the single-antenna observations were added to the data at the low frequency (408 MHz) but not at the high frequency (1240 MHz), a direct comparison of the two maps might lead to an erroneous spectral index distribution. To make a proper spectral index map, only the uv -spacings which are common to both observations are used. The spatial distribution of the spectral index between 0.408 and 1.4 GHz tends to flatten toward the center of the halo (Kim *et al.* 1987). We estimate that the spectral index is flattest near the halo center with the value of about 0.7 ± 0.2 , which is somewhat steeper than claimed by Dennison (1986). A much more definitive spectral index map, which incorporates 327 MHz WSRT data, will be published separately (Giovannini *et al.* 1990).

c) A Rotation Measure Probe of the Intracluster Magnetic Field

The purpose of this experiment is to search for Faraday rotation within the intracluster medium of the Coma Cluster which, combined with the X-ray data, could be used to estimate the strength and structure of the intracluster magnetic field. An early attempt to make this type of measurement was made by Dennison (1979). In a separate 12 hr run, we undertook multifrequency mapping of all possible sources within approx. 1.5 of the cluster center, in the knowledge that this was amply beyond the X-ray boundaries and, on any reasonable argument, at least the core region of the cluster's ICM. Eighteen different "target" radio sources were thus mapped, both "on" and "off" the Coma Cluster, down to a flux limit of 35 mJy. The sources were mapped in all Stokes parameters at four frequencies—1465, 1665, 4835, and 4885 MHz. The polarimetric calibration and the determination of ionospheric Faraday rotation were carried out in a similar way to the deep Coma map described in (b) above.

From the 18 multifrequency snapshots, we obtained Faraday rotation measures (RMs) of 17 sources in the field of the Coma Cluster. The best RM fits of the polarization data are listed and described in the Appendix. Figures 4a and 4b show two- and one-dimensional plots, respectively, of the source RMs relative to the center of the Coma Cluster, Abell 1656. These show reasonably convincingly that there is an excess rotation measure which is associated with the Coma Cluster of galaxies.

For the purpose of a simple statistical comparison, we have compared the RM statistics of sources inside and outside of a $35'$ radius circle centered on the cluster (Fig. 4a)—hereafter called "cluster" ($\theta_{cl} \leq 35'$) and "control" ($\theta_{cl} > 35'$) samples, respectively. The value $35'$ was chosen because it is close to the halo FWHM at the lowest measured frequency—30.9 MHz (Henning 1989), made with the Clark Lake Radio Telescope. The "cluster" sources are within, or behind, the cluster (but not in front). The dispersion, σ_{cl} , of the 10 "cluster" RM sources is 39 rad m^{-2} , about 5 times larger than σ_{con} of the "control" sample, which is 8.5 rad m^{-2} . This provides direct evidence for a magnetoionic medium associated with the Coma Cluster. The dispersion in RM arising from the magnetoionic medium, σ_c , is estimated to be

$$\sigma_c = \sqrt{\sigma_{cl}^2 - \sigma_{con}^2} \approx 38 \pm 6 \text{ rad m}^{-2}. \quad (1)$$

To provide a more formal statistical basis for this result (using the $35'$ circle), we undertook Monte Carlo simulations using the Ansari-Bradley W-test (Ansari and Bradley 1960) which is designed to detect a difference of scale parameters (e.g., variance) when the two underlying populations have a common median. RM values were selected at random from simulated Gaussian distributions having different σ values, and these distributions were added to the control sample for comparison. After performing 3000 such simulations, which produced a distribution of test statistic W^* values to compare with a critical value W_c^* for a given confidence level, we were able to set the upper and lower bounds to the "best" estimate of the excess RM generated by the Coma Cluster. The range, at the 84% confidence level, was found to be

$$30 < \sigma < 80 \text{ rad m}^{-2}.$$

When σ was adjusted to $\sim 45 \text{ rad m}^{-2}$, the two samples became statistically indistinguishable. As expected, the above

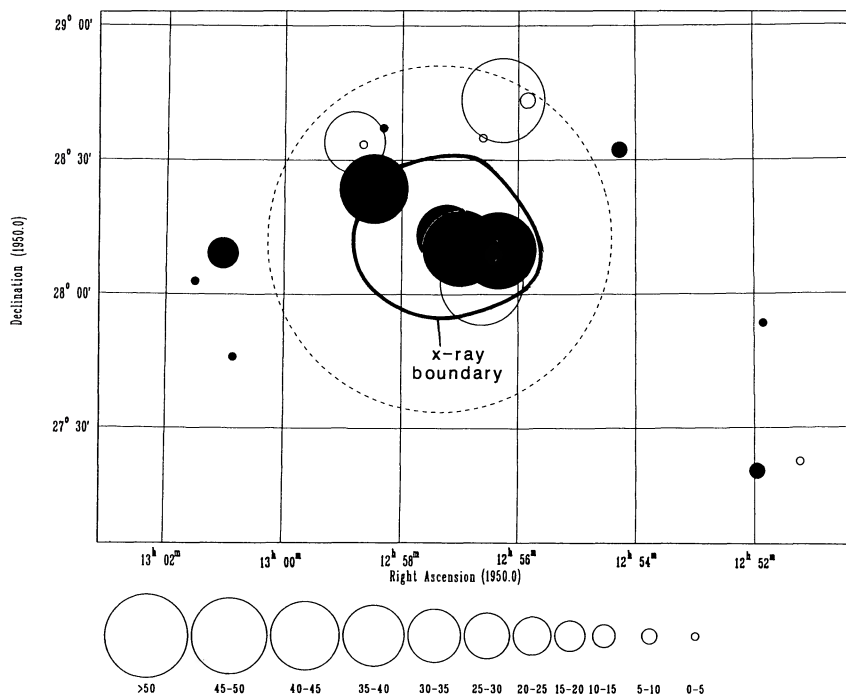


FIG. 4a

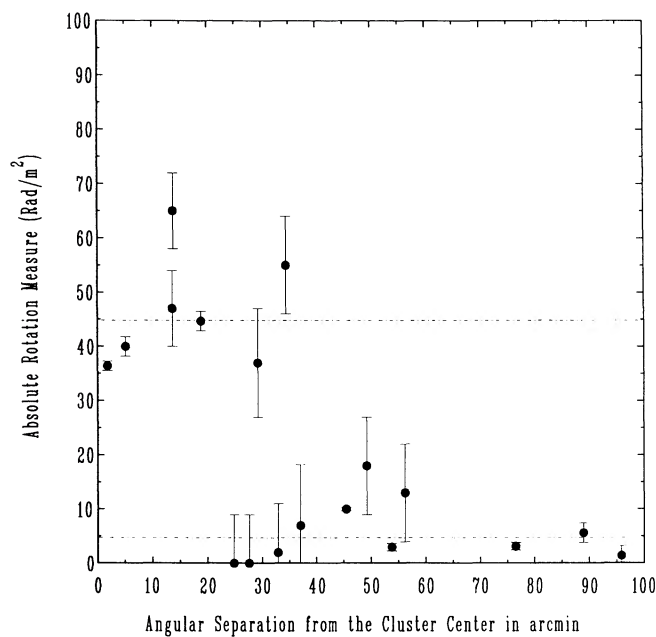


FIG. 4b

FIG. 4.—(a) The RM distribution is shown for 18 sources seen through the Coma Cluster and its vicinity. Filled and unfilled circles represent positive and negative RMs, respectively, and the sizes of circles are proportional to their absolute RM values, as shown in the bottom of the figure. The dashed circle is centered on the cluster and has a radius of $39'$, the Abell radius of the Coma Cluster. The solid line is the approximate boundary of the *Einstein* IPC X-ray source (see text). The rotation measure for the 18th source (3C 277.3) was obtained from other data (Kronberg 1988). (b) The *absolute* RM values of the radio sources in the Coma field are shown as a function of angular separation from the cluster center. The polarization data were obtained from the VLA in D-configuration. Foreground sources are all excluded from the sample.

confidence level varied with the set limits, and it increased if the 30–80 “window” is lowered. This test, using simulated populations of RMs, indicates that the σ_c in equation (1) properly represents the unbiased difference in the standard deviation of the two samples.

The statistical significance of the result is similar, or better if, instead of assuming a circular cluster core, we use another independently determined boundary—that defined by the lowest well-defined outer boundary of the *Einstein* X-ray image (0.56–3.5 keV), smoothed to $1'$ (FWHM) (D. E. Harris, private

communication). This boundary is also indicated in Figure 4a. Application of the Mann-Whitney “U” test (Mann and Whitney 1947), which avoids *a priori* assumptions about the nature of the RM distributions, gives a probability of only 0.002 that the five RMs within the X-ray boundary have the same “parent population” as the 13 RMs outside the X-ray boundary. Thus, we feel that the excess RM seen in the Coma Cluster is clearly detected in our data, although the modest number of sources available as RM probes obviously do not permit more than a “first-order” result.

A rough upper limit on any net *average* RM excess, either positive or negative, can be set at 30 rad m^{-2} . If this were associated with a cluster-sized, unidirectional field, such a field could be estimated from

$$\left(\frac{\text{RM}}{\text{rad m}^{-2}}\right) = 8.1 \times 10^5 \left(\frac{n}{\text{cm}^{-3}}\right) \left(\frac{H}{\mu\text{G}}\right) \left(\frac{L}{\text{Mpc}}\right), \quad (2)$$

to be less than $2 \times 10^{-8} \text{ G}$. Here we have used values of n and L from the X-ray data of Henriksen and Mushotzky (1986).

d) Search for Polarized Emission from the Halo Itself

In addition to the RM probe using background sources (c), we have attempted to map the polarized component of the central portion of the halo at both 1380 and 1630 MHz. The DRAO data had to be omitted for this experiment, since the 9 m DRAO antennae were not configured to map in linear polarization. For this reason, we cannot measure the polarized component of the entire halo emission, but only the central portion, which is dominated by 5C 4.81 and 5C 4.85. At a resolution of $1'$ (i.e., $\sim 40 \text{ kpc}$), no polarized emission was detected at either frequency to an upper limit of $500 \mu\text{Jy beam}^{-1}$. This corresponds to 1% of the strongest halo emission and 30% of the weakest emission in the VLA total intensity map.

III. THE INTRACLUSTER MAGNETIC FIELD AND ITS STRUCTURE

We now review the results of several different ways of inferring the strength and structure of the magnetic field of the intergalactic medium in the Coma Cluster, which we shall compare against our new, direct method described in § IIc. Briefly, these are (1) by making assumptions about equipartition between the magnetic and relativistic particle energy densities, (2) by estimating limits to the inverse Compton component of the halo X-ray emission, (3) by mapping the depolarization (and Faraday rotation) of the halo emission itself, and (4) using our new method described below.

Method (1) uses the assumption that energy equipartition prevails between the relativistic particles and the magnetic field. Then, from the measured luminosity ($L_{\text{halo}} = 2.2 \times 10^{41} h_{50}^{-2} \text{ ergs s}^{-1}$) and halo size, one can estimate the magnetic field which, for the Coma halo, is

$$H_{\text{eq}} \approx 0.5(1+k)^{2/7} \mu\text{G}, \quad (3)$$

where k is the (unknown) relativistic proton/electron energy ratio (Pacholczyk 1970). We note that letting k range from 10–100 changes the magnetic field estimate by only a factor of 2. The term h_{50} is the Hubble constant normalized to $50 \text{ km s}^{-1} \text{ Mpc}^{-1}$.

The estimate, or limit in case (2), is based on the fact that the same relativistic electrons responsible for the synchrotron emission in the halo will scatter microwave background photons to X-rays (Harris and Grindlay 1979). The inverse Compton (IC) component of the (otherwise thermal) X-ray emission has been limited to at most $\sim 10\%$ of the X-ray luminosity (Henriksen and Mushotzky 1986). This implies that the intracluster magnetic field strength should be $H_c > 0.2 \mu\text{G}$, or greater than $0.5 \mu\text{G}$ if the upper limit is 1%. These values are consistent with H_{eq} for reasonable values of k .

Method (3) was attempted, but we could not use it to estimate the magnetic field strength because polarized emission was not detected from the halo (see § II d). However, our measurements did allow us to deduce the scale size of the field

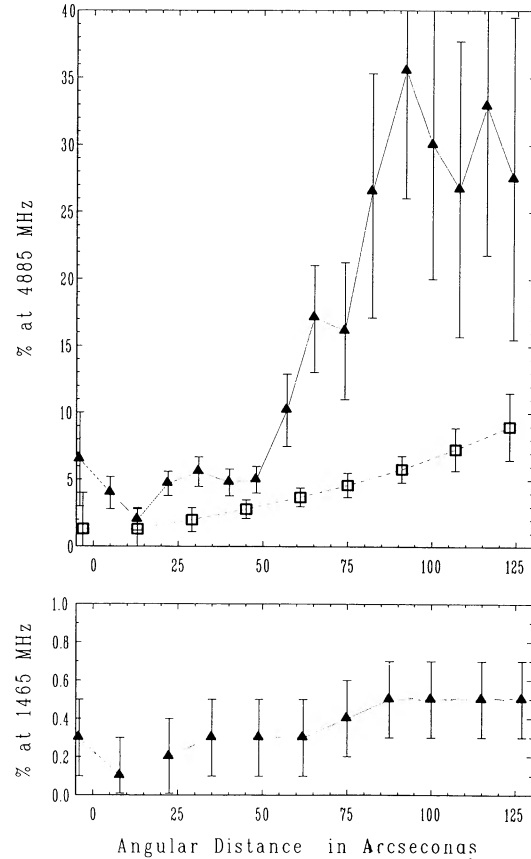


FIG. 5.—Variation of percentage polarization along the tail of the radio source 5C 4.81 at 4885 MHz (upper panel; filled triangles), and 1465 MHz (lower panel). The unfilled squares in the upper panel show the distribution of the percentage polarization at 4885 MHz after convolution to match the resolution at 1465 MHz. The two distributions are very different in that the maximum polarization at 4885 MHz is about 25%–30%, whereas it is below $\sim 1\%$ at 1465 MHz.

irregularities. When 5C 4.81 was observed at 4885 MHz with a synthesized beam of $21''.2$ ($= 13.8 \text{ kpc}$), the percentage polarization was found to be much higher. It ranges from 5% near the core to about 25%–30% in the tail (Fig. 5). The substantial polarization, especially in the tail, suggests that there is very little depolarization at 4885 MHz by differential Faraday rotation within the $21''$ beam. The 4885 MHz map was convolved to the resolution of the observations at 1.4 GHz, and the variation of percentage polarization was measured along the radio tail. The percentage polarization reaches a minimum of about 1% $10''$ from the center and thereafter increases monotonically along the radio tail to about 8% at $2'$ from the center. The beam depolarization, which is due to the structure in the polarized emission, appears to be significant.

Comparing the two 4885 MHz percentage polarization maps of different resolutions (see Fig. 6), the degree of beam depolarization appears to be more or less constant, about a factor of 2–3, along the radio tail. When the distributions of percentage polarizations at 4.9 and 1.4 GHz are compared at the same angular resolution, the depolarization factor varies from 10–20 over the radio tail (Fig. 5). The severity of the depolarization implies a disordered Faraday screen along the radio tail, as opposed to internal depolarization within the radio tail, and it suggests that the magnetic field is tangled on

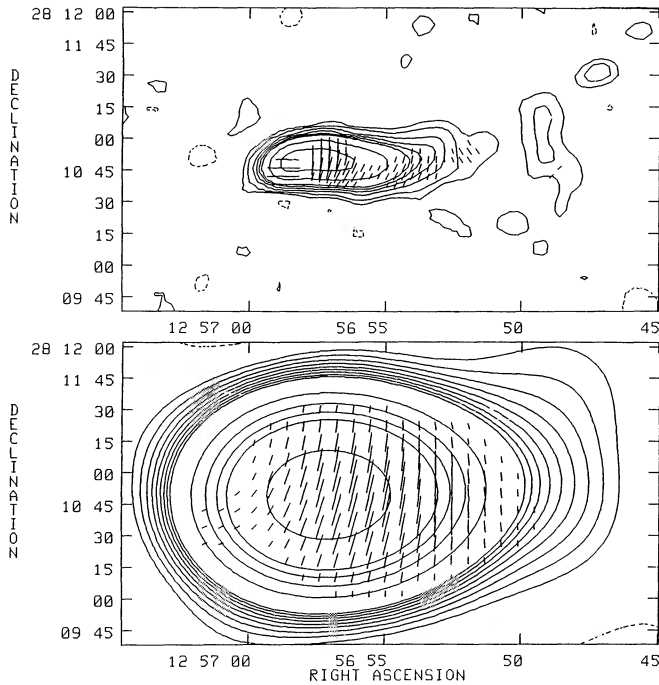


FIG. 6.—For 5C 4.81, contour map and polarization vectors are shown at 4885 MHz (*upper panel*). The resolution is about $21''$. The peak brightness is 23 mJy beam^{-1} , and contours are shown at $-0.4, 0.4, 0.8, 1.6, 2.4, 3.2, 4, 8,$ and 16 mJy beam^{-1} . The lines of polarized intensity are scaled such that $1''$ equivalent length = $0.125 \text{ mJy beam}^{-1}$. The lower panel shows the distribution of the polarized emission after convolving the upper map with a beamwidth of $1'$. The contour levels are at $-0.5, 0.5, 1, 1.5, \dots, 5, 10, 15, \dots, 25, 50, \text{ mJy beam}^{-1}$, and peak flux is 73 mJy beam^{-1} . The polarized intensity lines are scaled as above.

angular scales between $21''$ and $1'$. This tangling scale corresponds to a physical size range of $13\text{--}40 \text{ kpc}$, approximately the size of a galaxy, and we infer that this is characteristic of the intracluster field reversal scale.

We can now provide the most direct estimate of the intracluster magnetic field strength (method [4]), by combining our new Faraday rotation measures with the X-ray data, since the X-rays are presumably generated by the same electrons that produce the excess RM we have detected in the Coma Cluster.

Following the analysis of Lawler and Dennison (1982), the most probable value of H_c can be estimated as follows: for the case where there are many self-coherent Faraday cells along the line of sight through the cluster, the RM dispersion, σ_c , due to the magnetoionic medium in the cluster can be expressed as (Lawler and Dennison 1982)

$$\sigma_c = 760 \times \left(\frac{a}{0.5 \text{ Mpc}} \right) \left(\frac{n_0}{3 \times 10^{-3}} \right) \frac{H_c}{M^{1/2}} \times \frac{1}{[1 + (\langle \theta \rangle / \theta_c)^2]^{5/4}} \text{ rad m}^{-2}, \quad (4)$$

where H_c is the magnetic field strength of a cell in units of microgauss, M is the number of cells per X-ray core radius (θ_c), a is the linear core radius in units of 0.5 Mpc , n_0 is the central electron number density per cm^3 , and $\langle \theta \rangle / \theta_c$ is the average projected distance of the radio source from the cluster center as a fraction of the cluster core radius. Using $\theta_c \approx 10' \pm 1'$ (Abramopoulos and Ku 1983), $\langle \theta \rangle \approx 17' \pm 2'$, and a scale

parameter of $1' = 40 \text{ kpc}$ for Coma, then for $\sigma_c \approx 40 \text{ rad m}^{-2}$ (our result in this paper), we have

$$\frac{H_c}{M^{1/2}} = (0.33 \pm 0.13) \mu\text{G}. \quad (5)$$

The best observational and theoretical estimates indicate a cell size in the range $10\text{--}40 \text{ kpc}$ (see above and Jaffe 1980), yielding $M = 25 \pm 15$ cells per core radius. This gives

$$H_c = (1.7 \pm 0.9) \mu\text{G}. \quad (6)$$

It is noteworthy that this estimate is close to that deduced from equipartition arguments (method [1]). It thus provides an unusual opportunity to validate the widely invoked assumption of equipartition between relativistic particles and magnetic field in astrophysical relativistic plasmas. Our magnetic field estimates are also consistent with the lower limit based on the absence of significant inverse Compton-generated X-rays.

IV. THE RELATIONSHIP BETWEEN THE COMA X-RAY SOURCE AND THE RADIO HALO

The Coma Cluster is associated with a smooth, extended X-ray source of medium luminosity. The X-ray core radius is about $10'$ or less (Abramopoulos and Ku 1983), about the same size as the radio halo. However, the positions of the two sources are significantly displaced, the radio source being about $3'$ west of the X-ray source. In particular, there is an absence of radio emission along part of the eastern boundary of the X-ray halo. The position of the radio halo suggests that it is more likely to be associated with the subclump containing NGC 4874, one of the two D-type galaxies in the central region of the cluster, rather than the X-ray source.

The existence of this positional offset, viz. the absence of corresponding radio emission over part of the X-ray halo, suggests that the relativistic particles in the radio halo are not directly responsible for heating the X-ray-emitting gas. A possible mechanism for energy transfer between the two types of particles, Coulomb interactions, requires that the two sources be precisely coextensive. Also, a sufficiently high rate of Coulomb interactions would shorten the lifetime of the relativistic particles considerably (Lea and Holman 1978).

The halo is elongated approximately east-west, consistent with the shapes seen in both the galaxy distribution and the X-ray observations. However, the halo at 408 MHz shows structure unlike that of an elliptical Gaussian. A "tail"-like extension of the halo to the east is also visible in the 1380 MHz map. Both the 408 MHz and 1.4 GHz maps indicate that the radio halo is *more similar to the galaxy distribution than to the X-ray distribution*.

V. THE ORIGIN OF THE RADIO HALO

Several questions remain concerning the relativistic electrons in the radio halo: (1) What is the origin of the relativistic electrons? (2) What are their characteristic lifetimes? (3) Are they injected from some point source? (4) If so, can they be transported throughout the halo region without losing significant energy? (5) Independent of whether the injection source is in one place or distributed, does subsequent acceleration also take place? (6) If reacceleration of the electrons is needed to maintain their energy distribution, are proposed mechanisms in agreement with the observed size, spectral index, etc., of the halo source?

Four explanations have been advanced to explain the relativistic gas distribution in galaxy clusters. They are (a) diffusion from cluster radio sources, (b) relics of galaxies previously exhibiting head-tail behavior, (c) secondary electron models, and (d) turbulent galactic wakes (see Hanisch 1982; Valtaoja 1984 for a review). We briefly review various theories and data which could provide some answers to our six questions, and we show how our new results presented here point to some new answers.

An outward steepening of the spectral index might be expected on the basis of the following simple scenario: Particle reacceleration, if it exists, would not be as effective at the edge of the cluster as at the center, since the density of both intergalactic gas and galaxies, as well as the galaxy velocity dispersions, decrease outward from the cluster center (see Kent and Gunn 1982). Electrons at the edge are more likely to be "older" than at the center (i.e., a longer time has passed since the last energy input). Most loss mechanisms (e.g., synchrotron losses) result in a steepening of the energy spectrum and hence of the radio spectrum.

Another explanation for the *extent* of the radio halo is to postulate that it is a mosaic of the diffuse "fossil" tails of previous head-tail radio galaxies in which particle reaccelerations have, by and large, not occurred. From this theory, we might expect that the total extent of the radio halo should be *independent* of wavelength, i.e., there should be no systematic, large-scale variation of the spectral index. In addition, the "relic" theory is less likely to produce a smooth and centrally condensed profile of the radio halo—which is more or less what we observe.

It is intriguing that the two radio head-tail galaxies near the cluster center are separated by only $\sim 5'$, and that these two are the brightest radio sources. The radio halo center is near the most active of the two head-tail galaxies, 5C 4.81 (associated with an elliptical galaxy), the other 5C 4.85 being associated with a D-type galaxy. This suggests that these two galaxies are probably the primary source of the relativistic electrons which produce the halo.

We shall proceed on this hypothesis and examine the alternative particle production and acceleration theories mentioned above: the diffusion model is sensitively coupled to the *extent* of the radio halo. To explain the radio halo size, one requires a bulk diffusion velocity of $v_d \approx 10^3\text{--}10^4 \text{ km s}^{-1}$. This is a consequence of our determination of the intracluster magnetic field strength, $1\text{--}2 \mu\text{G}$, which causes a typical relativistic electron to lose half its energy through synchrotron radiation in approximately 10^8 yr . In the absence of *in situ* particle reacceleration, the diffusion theory has the following problem: If $v_d \geq 10^3 \text{ km s}^{-1}$, 5C 4.81, the likeliest candidate for the source of relativistic electrons at 2.6×10^{58} particles per 10^8 yr , falls short by a factor of 10 from what is needed to supply the Coma halo. We assume that the above rate was constant for 10^9 yr . Note that the maximum lifetimes of relativistic electrons radiating near 1 GHz are only about 10^8 yr and are limited increasingly by the inverse Compton losses as the local field strengths drop below about $3 \mu\text{G}$. In addition, diffusion velocities significantly above 10^3 km s^{-1} , being supersonic, would be associated with either jets or strong shocks, for which there is little evidence in our Coma halo map—at least down to the resolution corresponding to a galaxy size.

Conversely, if $v_d \leq 10^2 \text{ km s}^{-1}$, the electrons will lose their energy before reaching the outer halo, and we cannot explain its observed extent. Diffusion alone cannot explain the

observed radio halo. It needs to be accompanied by particle reacceleration.

The secondary electron model (Dennison 1980) attempts to explain the extent and the steep spectral index of the radio halo. The virtue of this model is that *primary protons* survive for time periods of order 10^{10} yr in the radio halo since, unlike the primary electrons, they are not as susceptible to synchrotron or inverse Compton losses. Thus, they escape from radio galaxies and diffuse over distances $\sim 1 \text{ Mpc}$ over time periods of about 10^{10} yr in the intracluster medium before suffering inelastic collisions with thermal protons. While the predicted overall spectral index and luminosity of the radio halo agree well with what has been observed, the spectral index steepening in the outer halo is found to disagree with the predictions of this model.

We now consider the fourth model (d)—the formation of turbulent wakes behind galaxies moving through the ICM. While it cannot be considered unambiguously proven by observations, it is widely believed that wakes are likely to be turbulent if the ICM is magnetized, as we have confirmed it to be. The turbulent nature of the wakes stems from the very large Reynolds numbers which are characteristic of the galaxy-ICM interaction. The relevant hydrodynamic and magnetic Reynolds numbers (De Young 1980) are $R \approx 6 \times 10^{24}$ and $R_m \approx 7.7 \times 10^{26}$, respectively, for the parameters of the ICM of the Coma Cluster of galaxies which are deduced from the present radio (and X-ray) data. We would expect, therefore, that a fully developed turbulence exists on virtually all scales up to the characteristic size of a galaxy in the trailing wakes.

If we adopt the argument that the galactic wakes are turbulent (because of the very large Reynolds number), then they are able to reaccelerate particles via the Eilek-Henriksen mechanism (Eilek and Henriksen 1984). The volume filling factor of the wakes is crudely estimated to be of order 0.1 in the region near the cluster center. This implies a total power input in reaccelerated relativistic particles of about $10^{41} \text{ ergs s}^{-1}$, which is in good agreement with the observed radio halo luminosity (see Kim 1988).

The filling factor estimate is derived, following Jaffe's (1980) analysis, from the estimate of the distance from the center of a moving galaxy χ_A , at which the velocity at the end of the turbulence cascade equals the Alfvén velocity, v_A . The volume occupied by the wake of a galaxy is

$$V_w \approx \frac{3\pi}{5} r_g^3 \left(\frac{v_g}{v_A} \right)^{5/2}, \quad (7)$$

(where r_g , v_g are the radius and velocity of the galaxy). This corresponds to a sphere of radius $\approx 35 \text{ kpc}$. Since the turbulence requires a certain time to be fully developed (about 100 kpc from a moving galaxy in Coma), V_w should be reduced somewhat, with a corresponding reduced estimate for $r_{\text{eff}} \approx 30 \text{ kpc}$. Now the volume filled by wakes *within the core region* is $V_w N_g$, so that the mean volume filling factor of wakes is $f_w \approx 3V_w N_g / 4\pi r_c^3$, where r_c is the radius of the cluster core region. From optical studies (Quintana 1979; Kent and Gunn 1982, and references therein), the number of galaxies brighter than $V_{26} = 16 \text{ mag}$ within the core is about 50 (it will exceed 100 if the limiting magnitude goes down to 18th, which is reasonable for Coma). Thus the volume filling factor f_w should be (for $r_c = 300 \text{ kpc}$ and $r_{\text{eff}} = 30 \text{ kpc}$) $\approx (30/300)^3 \times 100$ which is 0.1. (It could indeed be more than 0.1 if many dwarf galaxies

[fainter than 18 mag] exist in the core and are equally capable of producing wakes.)

We note, however, that there is no direct morphological evidence for features which could be convincingly associated with galactic wakes even after filtering out the large-scale components of the halo emission. The lack of any visible fine structure also suggests that the magnetic field *contrast* in the halo is small, at least on the scale of a galaxy. It also suggests, though does not prove, that the volume filling factor is not excessively small. Given the large uncertainty in the parameters associated with the galactic wakes, including the uncertain wake filling factor, the radio morphology alone cannot either support or rule out the galactic wake theory. However, we can conclude that with an efficient particle acceleration mechanism, such as in turbulent wakes, neither large diffusion coefficients nor high bulk diffusion speeds are required to explain the extent of the halo. Particle reacceleration tends to counteract the radiation losses over much of the halo region.

VI. CONCLUDING REMARKS

We have presented the most detailed image of the intergalactic halo yet seen in a cluster of galaxies. By using faint background radio sources as “Faraday probes,” detecting and

defining the excess Faraday rotation from the intracluster gas, and combining this with the *Einstein* X-ray data, we have obtained one of the most direct measurements made to date of the magnetic field strength in intergalactic space. Our estimate provides us with a rare opportunity in extragalactic astronomy to perform an independent check of the widely used assumption of equipartition between relativistic particles and magnetic field.

It seems reasonable to conclude that particle reacceleration in the ICM is the key to the origin of the radio halo. We propose that reacceleration in an ICM requires a sufficiently strong magnetic field in the medium, and this determines whether a cluster exhibits a radio halo.

We thank the staff of the NRAO Very Large Array for their assistance and support, and D. E. Harris for communicating *Einstein* X-ray data. We also thank L. E. M. Carriere for her assistance in the preparation of this paper, and some helpful suggestions from an anonymous referee. This research was supported in part by the Natural Sciences and Engineering Research Council of Canada (NSERC) (P. P. K.), and by the University of Toronto (K. T. K.).

APPENDIX

COMMENTS ON THE FIT OF THE ROTATION MEASURES

For RM fitting of the polarization data, a routine “NPI” written by R. Mably was used. This performed a systematic search for best least-squares fits over the range $-1000 \leq \text{RM} \leq +1000 \text{ rad m}^{-2}$.

The $n\pi$ ambiguity in the polarization position angles used to determine the RMs of these sources can be reasonably eliminated, since two of the frequencies used, 1465 and 1665 MHz, are close to each other. In Table 1, the best RM estimates of 18 radio sources are summarized, and the distribution of the absolute RM values is shown in Figures 4a and 4b. For nine sources, only the two nearby wavelengths were used, in which case the *minimum* RM is indicated. The next possible $n\pi$ ambiguity would give an improbably large RM, of order 300 rad m^{-2} which is very unlikely in this region of the galactic RM sky (Simard-Normandin, Kronberg, and Button 1981). The dispersions of the Faraday rotation measures of the two samples show a clear difference, and this is well illustrated in the figures. Table 2 contains a statistical comparison of these two groups.

TABLE 1
ROTATION MEASURES OF THE SOURCES IN THE COMA FIELD

Source Name	θ_{cl}	RM (rad m^{-2})	Intrinsic Position Angle	Notes ^a
5C 4.13	95.9	-1 ± 2	$133^\circ \pm 3^\circ$	
5C 4.20	88.9	6 ± 2	135 ± 3	
5C 4.42	45.4	10 ± 2	-7 ± 1	
5C 4.61	37.0	-7 ± 11	37 ± 20	
5C 4.68	34.4	-55 ± 9	...	1
5C 4.70	13.6	47 ± 7	...	1
5C 4.74	13.8	-65 ± 7	...	1
5C 4.75	24.8	0 ± 9	...	1
5C 4.81	5.1	-49 ± 11	4 ± 3	2
		-350 ± 7	132 ± 3	2
5C 4.85	1.9	-32 ± 10	39 ± 17	2
		174 ± 7	5 ± 9	2
5C 4.114	18.8	45 ± 2	12 ± 3	
5C 4.112a	27.6	0 ± 9	...	1
5C 4.112b	29.2	-37 ± 10	...	1
5C 4.127	32.9	-2 ± 9	...	1
5C 4.152A	53.8	3 ± 1	-47 ± 1	3
5C 4.154	49.2	18 ± 9	...	1
5C 4.158	56.2	13 ± 9	...	1
3C 277.3	76	3 ± 1	...	

^a NOTES.—(1) Minimum RM is used when the polarization data available cover less than three frequencies. (2) See text. (3) Other name of this source is 1300 + 27W2A.

TABLE 2
ROTATION MEASURE STATISTICS OF SOURCES IN THE COMA FIELD^a

Sample	Cluster ^b	Control ^c	Comments
Number of Sample	10	7	
Mean Rotation Measure ^d	-14.8 ± 12.5 27.1 ± 1.5	5.8 ± 3.2 3.4 ± 0.6	Unweighted ^e Weighted ^e
Dispersion ^{d,f}	39.5	8.5	

^a Foreground sources are excluded from the samples.

^b Angular separation from the cluster center of the sources is $\theta_{cl} \leq 35'$.

^c Sources with $\theta_{cl} > 35'$.

^d Rotation measure in units of rad m^{-2} .

^e Statistical weight.

^f Weighted and unweighted cases are similar.

I. NOTES ON SOME INDIVIDUAL RM DETERMINATIONS

5C 4.81: Only the polarization data of the head were used. There are two RMs equally likely to fit the data: $\text{RM} = -349.5 \pm 6.5$ ($\chi_0 = 60 \pm 13$), $\text{RM} = -49.2 \pm 10.5$ ($\chi_0 = 13 \pm 22$). Here χ_0 is the intrinsic position angle (IPC). The χ^2 test indicated that the former fit is only slightly better than the latter. *5C 4.85*: There are three more possible RMs other than the value listed in Table 1: $\text{RM} = 174 + 7$ ($\chi_0 = 5 \pm 9$), $\text{RM} = -348 \pm 17$ ($\chi_0 = 126 \pm 21$), and $\text{RM} = -543 \pm 7$ ($\chi_0 = 152 \pm 12$). The χ^2 test indicated that the first value in the list is superior to the rest. *5C 4.13*: $\text{RM} = -549 \pm 2$ ($\chi_0 = 64 \pm 3$) also fits the data. *5C 4.20*: $\text{RM} = -537 \pm 2$ ($\chi_0 = 66 \pm 3$) also fits the data. *5C 4.42*: Two RMs fit the data equally well: $\text{RM} = -320 \pm 1$ ($\chi_0 = 340 \pm 1$) and $\text{RM} = 340 \pm 1$. *5C 4.61*: Two RMs equally fit the data: $\text{RM} = 306 \pm 2$ ($\chi_0 = 158 \pm 4$) and $\text{RM} = -237 \pm 1$ ($\chi_0 = 89 \pm 1$). *5C 4.114*: $\text{RM} = -68 \pm 3$ ($\chi_0 = 35 \pm 5$) also fits the data.

REFERENCES

- Abramopoulos, F., and Ku, W. H.-M. 1983, *Ap. J.*, **271**, 446.
 Ansari, A. R., and Bradley, R. A. 1960, *Ann. Math. Stat.*, **31**, 1174.
 Ballarati, B., Feretti, L., Ficarra, A., Gavazzi, G., Giovannini, G., Nanni, M., and Olori, M. C. 1981, *Astr. Ap.*, **100**, 323.
 Bozyan, E. P. 1968, *Ap. J. (Letters)*, **152**, L155.
 Bridle, A. H., Fomalont, E. B., Miley, G. K., and Valentijn, E. A. 1979, *Astr. Ap.*, **80**, 201.
 Bridle, A. H., and Purton, C. R. 1968, *A.J.*, **73**, 717.
 Cordey, R. A. 1985, *M.N.R.A.S.*, **215**, 437.
 Dennison, B. 1979, *A.J.*, **84**, 725.
 ———. 1980, *Ap. J. (Letters)*, **239**, L93.
 ———. 1986, *Astr. Ap.*, **159**, 251.
 De Young, D. S. 1980, *Ap. J.*, **241**, 81.
 Eilek, J. A., and Henriksen, R. N. 1984, *Ap. J.*, **277**, 820.
 Erickson, W. C., and Cronyn, W. M. 1965, *Ap. J.*, **142**, 1156.
 Gavazzi, G., and Trinchieri, G. 1983, *Ap. J.*, **270**, 410.
 Giovannini, G., Feretti, L., Kim, K.-T., and Kronberg, P. P. 1990, in preparation.
 Gisler, G. R., and Miley, G. K. 1979, *Astr. Ap.*, **76**, 109.
 Gubanov, A. G. 1982, *Astrophysics*, **18**, 107.
 Hanisch, R. J. 1980, *A.J.*, **85**, 1565.
 ———. 1982, *Astr. Ap.*, **116**, 137.
 Hanisch, R. J., and Erickson, W. C. 1980, *A.J.*, **85**, 183.
 Harris, D. E., and Grindlay, J. E. 1979, *M.N.R.A.S.*, **188**, 25.
 Harris, D. E., Kapahi, V. K., and Ekers, R. D. 1980, *Astr. Ap. Suppl.*, **39**, 215.
 Harris, D. E., and Miley, G. K. 1978, *Astr. Ap. Suppl.*, **34**, 117.
 Haslam, C. G. T., Salter, C. J., Stoffel, H., and Wilson, W. E. 1982, *Astr. Ap. Suppl.*, **47**, 1.
 Henning, P. A. 1989, *A.J.*, **97**, 1561.
 Henriksen, M. J., and Mushotzky, R. F. 1986, *Ap. J.*, **302**, 287.
 Jaffe, W. J. 1980, *Ap. J.*, **241**, 925.
 Jaffe, W. J., and Rudnick, L. 1979, *Ap. J.*, **233**, 453.
 Kent, S. M., and Gunn, J. E. 1982, *A.J.*, **87**, 945.
 Kim, K.-T. 1988, Ph.D. thesis, University of Toronto.
 Kim, K.-T., Kronberg, P. P., Dewdney, P. E., and Landecker, T. L. 1987, in *Continuum Radio Processes in Clusters of Galaxies*, ed. C. O'Dea and J. Uson (Green Bank: NRAO), p. 199.
 Kronberg, P. P. 1988, unpublished.
 Lawler, J. M., and Dennison, B. 1982, *Ap. J.*, **252**, 81.
 Lea, S. M., and Holman, G. D. 1978, *Ap. J.*, **222**, 29.
 Mann, H. B., and Whitney, D. R. 1947 *Ann. Math. Stat.*, **18**, 52.
 Pacholczyk, A. G. 1970, *Radio Astrophysics* (San Francisco: Freeman).
 Pauliny-Toth, I. I. K., Wade, C. M., and Heesch, D. S. 1969, *Ap. J. Suppl.*, **13**, 65.
 Quintana, H. 1979, *A.J.*, **84**, 15.
 Roger, R. S., Costain, C. H., and Lacey, J. D. 1969, *A.J.*, **74**, 366.
 Roger, R. S., Costain, C. H., Lacey, J. D., Landecker, T. L., and Bowers, F. K. 1973, *Proc. IEEE*, **61**, 1270.
 Schlickeiser, R., Sievers, A., and Thiemann, H. 1987, *Astr. Ap.*, **182**, 21.
 Sievers, A. 1986, private communication.
 Simard-Normandin, M., Kronberg, P. P., and Button, S. 1981, *Ap. J. Suppl.*, **46**, 239.
 Smith, M. A. 1968, Ph.D. thesis, University of Cambridge.
 Valentijn, E. A. 1978, *Astr. Ap.*, **68**, 449.
 Valtaoja, E. 1984, *Astr. Ap.*, **135**, 141.
 Veidt, B. G., Landecker, T. L., Vaneldik, J. F., Dewdney, P. E., and Routledge, D. 1985, *Radio Sci.*, **20**, 1118.
 Viner, M. R., and Erickson, W. C. 1973, *A.J.*, **80**, 931.
 Williams, P. J. S., Kenderdine, S., and Baldwin, J. E. 1966, *Mem. R.A.S.*, **70**, 53.
 Willson, M. A. G. 1970, *M.N.R.A.S.*, **151**, 1.

P. E. DEWDNEY and T. L. LANDECKER: Dominion Radio Astrophysical Observatory, National Research Council, P.O. Box 248, Penticton, BC, Canada V2A 6K3

K.-T. KIM and P. P. KRONBERG: Department of Astronomy, University of Toronto, Toronto, Ontario, Canada M5S 1A7